Frontiers of Information Technology & Electronic Engineering
www.jzus.zju.edu.cn; engineering.cae.cn; www.springerlink.com
ISSN 2095-9184 (print); ISSN 2095-9230 (online)
E-mail: jzus@zju.edu.cn

Traditional soliton erbium-doped fiber laser with InSe as saturable absorber*

Xiaojuan LIU[1], Guomei WANG[1,2], Mingxiao ZHU[1],
Kezhen HAN[1], Wenfei ZHANG[†‡1,2], Huanian ZHANG[†‡1,2]

[1]*School of Physics and Optoelectronic Engineering, Shandong University of Technology, Zibo 255000, China*
[2]*Collaborative Innovation Center of Light Manipulations and Applications, Shandong Normal University, Jinan 250358, China*
[†]E-mail: zhangwenfei@sdut.edu.cn; huanian_zhang@163.com

Received July 29, 2020; Revision accepted Sept. 29, 2020; Crosschecked Dec. 18, 2020; Published online Jan. 29, 2021

Abstract: Indium selenide (InSe) is a typical layered metal-chalcogenide semiconductor that has potential for developing ultrafast optoelectronic devices. In this work, InSe-polyvinyl alcohol (InSe-PVA) film is employed as saturable absorber and prepared by mixing InSe nanosheets solution and polyvinyl alcohol solution. The nonlinear absorption properties of the InSe saturable absorber (InSe-SA) are investigated, showing that the nonsaturable absorption and modulation depth are 37.5% and 9.55%, respectively. Traditional soliton lasers are generated in erbium-doped fiber (EDF) laser-employed InSe as a mode-locker. The central wavelength and pulse duration of the traditional soliton pulse are 1568.73 nm and 2.06 ps, respectively, under a repetition rate of 1.731 MHz. The maximum average output power is 16.4 mW at the pump power of 413 mW. To the best of our knowledge, this is the first demonstration of a traditional soliton pulse with InSe as a mode-locker. The experimental results further demonstrate that InSe is an outstanding nonlinear absorption material in ultrafast fiber laser.

Key words: Fiber laser; Nanosheets; Traditional soliton
https://doi.org/10.1631/FITEE.2000387 **CLC number:** O437

1 Introduction

Two-dimensional (2D) materials exhibit distinct properties of electric conductivity, mechanics, and optics compared with traditional materials. These unique and layer-dependent optical properties, such as the high damage threshold, fast response recovery, and excellent nonlinear property, have attracted particular attention for ultrafast optoelectronic devices. Benefitting from these advantages, pulsed fiber laser, which has been widely used in the fields of industrial manufacturing (Huang D et al., 1991) and biomedicine (Chen JM et al., 2020; Xie et al., 2020), and in scientific research (Goda and Jalali, 2013), is typically applied in the field of 2D materials (Huang WC et al., 2018, 2019; Ge et al., 2019; Guo B et al., 2019; Guo SY et al., 2019). Graphene was the first developed and thoroughly investigated 2D material. In 2009, it was first demonstrated as saturable absorber (SA) for generating fiber laser (Bao et al., 2009; Zhang H et al., 2009). The application of graphene has inspired the full development of 2D materials as SA. In the past decade, a series of 2D materials, including topological insulators (TIs) (Liu H et al., 2014; Sotor et al., 2014a; Guo QX et al., 2019; Xu NN et al., 2019), MXene (Jhon et al., 2017; Jiang et al., 2018; Sun et al., 2018; Wu Q et al., 2019; Wang C et al., 2020), transition metal dichalcogenides (TMDs) (Liu WJ et al., 2017; Niu et al., 2017, 2018; Wu LM et al., 2018; Hu et al., 2019; Liu JS et al., 2019; Xie et al., 2019; Li L et al., 2020; Ma et al., 2020; Wang GM et al., 2020; Zhang HN et al., 2020), and various monoelemental materials (Xene) (black phosphorus

‡ Corresponding authors
* Project supported by the National Natural Science Foundation of China (Nos. 11904213, 11704226, and 11704227)
ORCID: Wenfei ZHANG, https://orcid.org/0000-0002-4408-4352

(BP) (Sotor et al., 2014b; Chen Y et al., 2015; Song et al., 2016), such as graphdiyne (Zhao et al., 2019), phosphorene (Luo et al., 2015; Li D et al., 2015; Xu YH et al., 2017; Mao et al., 2018), antimonene (Song et al., 2017; Liu GW et al., 2019), bismuthene (Guo B et al., 2018; Lu et al., 2018; Wang C et al., 2019), silicone (Xing et al., 2017; Wang MX et al., 2019; Liu GW et al., 2020), and tellurene (Guo J et al., 2019; Xu NN et al., 2020; Zhang WF et al., 2020), have been developed as SA and exhibit favorable performance.

Indium selenide (In_2Se_3 or InSe), which is a typical III-V group metal-chalcogenide compound (MX or M_2X_3), has a structure of Se-In-Se-In-Se quintuple layers (In_2Se_3) or four covalently bonded Se-In-In-Se atomic planes (InSe) (Mudd et al., 2013; Feng et al., 2016). The adjacent layers are bonded through van der Vaals interactions, which indicates that nanosheets are prepared by mechanical exfoliation or the liquid phase exfoliation (LPE) method. Additionally, bandgap has a remarkable layer-dependent property that varies from 1.45 to 2.8 eV (In_2Se_3) (Quereda et al., 2016) or from 1.2 to 1.4 eV (InSe) (Lei et al., 2014).

Indium selenide has experimentally demonstrated strong nonlinear absorption properties and has been widely developed as SAs for generating ultrafast pulsed fiber lasers. In 2018, In_2Se_3 nanosheets were mechanically exfoliated from α-In_2Se_3 crystal and directly transferred into a fiber ferrule to serve as a mode-locker for achieving Tm-doped fiber laser (Ahmad et al., 2018a). The generated mode-locked pulse duration was 5.79 ps at a repetition rate of 6.93 MHz. In another work, the passively Q-switched operation was achieved based on In_2Se_3 as SA (Ahmad et al., 2018b), and the generated pulse can be tuned from 1533 to 1573 nm. Yan et al. (2018) prepared In_2Se_3 via the magnetron-sputtering deposition method. Passively mode-locked fiber lasers were successfully generated by employing fabricated α-In_2Se_3 as SAs operating at 1.5 and 2 μm. Wang GM et al. (2019) demonstrated a wavelength-switchable vector-soliton fiber laser. The central wavelength can be switched from 1558 to 1530 nm. Meanwhile, the applications of InSe have been under investigation. Yang et al. (2018) reported passively Q-switched and mode-locked erbium-doped fiber (EDF) lasers based on InSe as SAs. The pulse repetition rate varied over a range of 5.58 to 13 kHz under Q-switched operation, and the pulse duration was 2.96 ns with a repetition rate of 1.74 MHz under mode-locked operation. In another contribution, employing InSe as SA, the stable mode-locked operation was achieved with a maximum pulse energy of 9.26 nJ at a repetition rate of 1.76 MHz in a Yb-doped fiber laser (Xu NN et al., 2018). Fu et al. (2019) reported an InSe-based large-energy mode-locked EDF laser. In this case, the maximum pulse energy was as high as 20.4 nJ with a repetition rate of 586.3 kHz. Previous studies proved that indium selenide (In_2Se_3 and InSe) exhibited favorable performance for SAs in generating pulsed fiber lasers. However, compared with other 2D materials, such as graphene, MXenes, and TMDs, potential applications have not been investigated, such as the generation of traditional soliton (TS) and dissipative soliton (DS) pulses.

In this study, InSe-polyvinyl alcohol (InSe-PVA) film is fabricated by desiccation after blending InSe nanosheets solution and PVA solution. The nonlinear saturable absorption properties are further investigated using a power-dependent system. The nonsaturable absorption, modulation depth, and saturation intensity are 37.5%, 9.55%, and 1.68 MW/cm^2, respectively. An EDF laser is constructed by sandwiching the InSe-PVA film between two fiber ferrules as SA. The TS pulses are generated with a pulse duration of 2.06 ps under a repetition rate of 1.731 MHz. This is the first demonstration of TS operation employing InSe as SA. The experimental results verify that InSe is significant in developing new ultrafast photonic devices.

2 Preparation and characterization of InSe-SA

2.1 Preparation of InSe-SA

Generally, the fabrication of InSe-SA includes two steps: fabrication of few-layer InSe nanosheets and fabrication of InSe-SA. In our experiment, the dispersion solution of InSe nanosheets is purchased (Haolai Tech., China) (Fig. 1a). The InSe nanosheets are prepared using the LPE method, which is the dominant method for preparation of 2D materials. The procedure for the fabrication of InSe-SA is shown in Fig. 1b. The InSe nanosheets solution and PVA solution (w(PVA)=5%) are blended at a volume ratio of 1:1. Then, the hybrid InSe-PVA solution is stirred for 1 h to obtain a uniform InSe-PVA solution in a magnetic stirrer. Finally, we drop the hybrid InSe-PVA solution on a clean plastic substrate for desiccation. After desiccation under 25 °C for 72 h, a piece of thin InSe-PVA film is formed. This thin film is the desired InSe-SA.

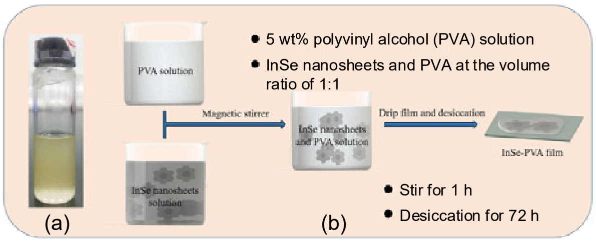

Fig. 1 The image of commercial InSe nanosheets dispersion solution (a) and the procedure for the fabrication of InSe-SA (b)

2.2 Characterization of InSe and InSe-SA

Raman spectrometry (HR Evolution, Horiba Scientific, Japan), X-ray diffraction (XRD, SmartLab, Rigaku, Japan), scanning electron microscopy (SEM, Sigma HD, Zeiss, Germany), energy-dispersive X-ray spectroscopy (EDS, Oxford Instruments, UK), and atomic force microscopy (AFM, Dimension Icon, Bruker, Germany) were introduced to verify the quality and properties of the InSe nanosheets, and the measurement results are shown in Fig. 2. The Raman property is measured using a 532 nm laser source under room temperature for InSe nanosheets. As shown in Fig. 2a, three observed Raman peaks correspond to 116.3, 173.7, and 226 cm^{-1}, respectively, which are consistent with the reported results (Mudd et al., 2013; Feng et al., 2016; Quereda et al., 2016). The XRD measurement of InSe nanosheets is shown in Fig. 2b. The diffraction peaks, i.e., (002), (004), (006), (008), and (110), are identical to the standard pattern of InSe (JPCDS No. 34-1431). Raman spectrum and XRD indicate that the prepared InSe-SA shows high purity and good quality. The SEM and EDS results are shown in Figs. 2c and 2e, respectively. The SEM image depicts that the nanosheets possess a minimal layered structure. The EDS result reveals that only In and Se exist in the measured sample, which further confirms the purity of InSe nanosheets. Fig. 2d shows the AFM image. The thickness and profiles corresponding to line 1 and line 2 are shown in Fig. 2f. The profiles reveal that the thickness of the InSe nanosheets is approximately 15 nm, which corresponds to approximately 20 layers of InSe.

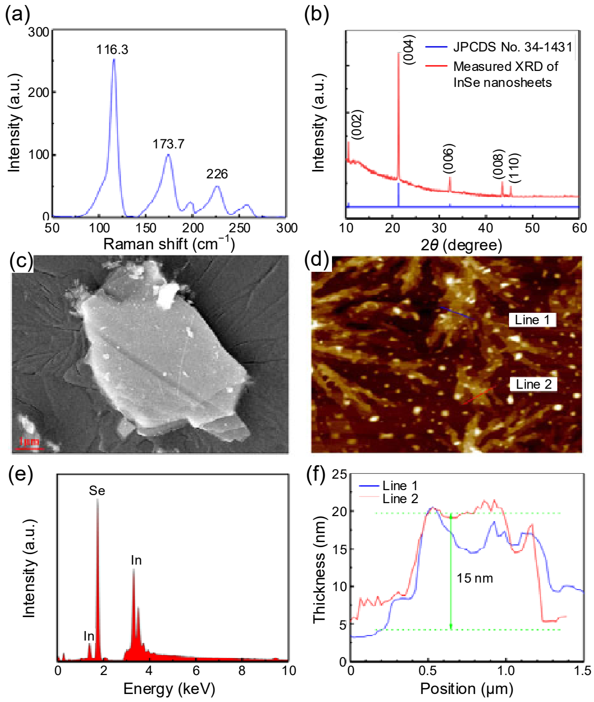

Fig. 2 Raman spectrum of the InSe nanosheets (a), measurement and theoretical XRD results of InSe nanosheets (b), SEM image of InSe nanosheets (c), AFM image of InSe nanosheets (d), EDS result of InSe nanosheets (e), and thickness and profiles of InSe nanosheets (f)

The nonlinear saturable properties of SA are decisive in the performance of the proposed fiber laser and have been systematically investigated. The measurement system is shown in Fig. 3a. The pulse source is a homemade fiber laser, and the central wavelength, pulse duration, and repetition rate of the incident laser are 1564.8 nm, 0.97 ps, and 12.5 MHz, respectively. First, an optical attenuator is inserted to continuously adjust the input power of the incident light. Then, the incident laser beam is divided into two beams using an 80:20 output coupler (OC). After passing through the InSe-SA, the larger one is received by detector I. The smaller one is directly measured by detector II as the reference. The varying transmission of InSe-SA according to the input power is displayed as the dot in Fig. 3b. The experimental data are fitted using the two-level saturable absorption model (Bao et al., 2009):

$$T(I)=1-\left(\frac{\alpha_s}{1+I/I_{sat}}+\alpha_{ns}\right),$$

where $T(I)$ is the transmission of the InSe-SA, I the power of the incident pulse, I_{sat} the saturation intensity, and α_s and α_{ns} the modulation depth and nonsaturable absorption, respectively. The fitted line is shown as the solid curve in Fig. 3b. After curve fitting, the nonsaturable absorption, modulation depth, and saturation intensity are 37.5%, 9.55%, and 1.68 MW/cm^2, respectively. The results indicate that the InSe-SA shows typical characteristics of saturable absorption.

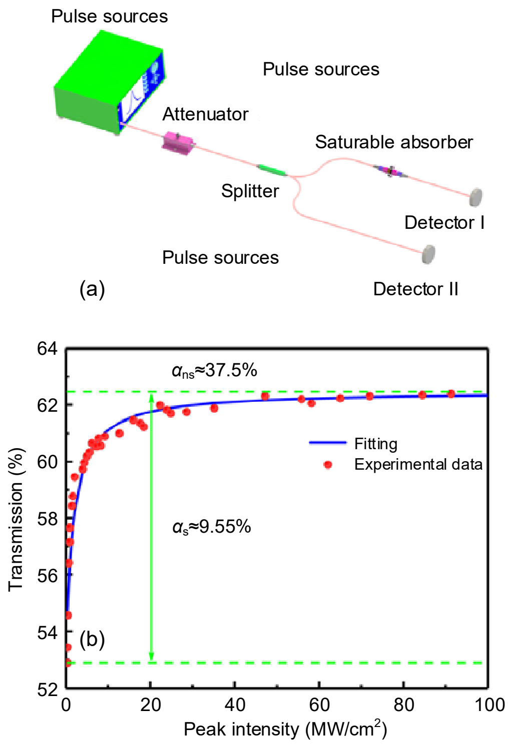

Fig. 3 Typical system schematic for measuring saturable absorption properties (a) and the measured and fitted nonlinear absorption property of InSe-SA (b)

3 Fiber laser setup

The schematic of the proposed fiber laser setup is shown in Fig. 4. The pump source is a laser diode (LD) centered at 976 nm. The 980/1550 nm wavelength division multiplexer (WDM) is employed to couple the pump source to the ring cavity. A piece of 9 m long EDF (MP980), whose dispersion value is −18 ps/nm/km, is employed as the laser gain medium. A polarization controller (PC) is used to adjust the polarization state of the cavity. The unidirectional propagation of the light in the ring cavity is ensured by a polarization-independent isolator (PI-ISO). A 10/90 OC is inserted to extract the testing signal for various measurements. The InSe-SA is sandwiched between two fiber ferrules that are inserted into the ring cavity. A piece of 100 m long single mode fiber (SMF) (SMF-28), whose dispersion value is 17 ps/nm/km, is employed to adjust the total dispersion of the ring cavity. The pigtail fiber of other elements is SMF-28. The total length of the ring cavity is approximately 118.7 m. Thus, the net dispersion of the total cavity is calculated as approximately −2.17 ps^2. The characteristics of the output pulse, including the spectrum, pulse train, pulse duration, repetition rate, and average output power, are monitored by an optical spectrum analyzer (AQ6370B, YOKOGAWA, Japan), an autocorrelator (FR-103XL, FEMTOCHROME, USA), a digital oscilloscope (DPO4054, Tektronix, USA), a radio frequency spectrum analyzer (RF) (FPC1000, R&S, Germany), and a power meter (GR-103A, ZEYE, China).

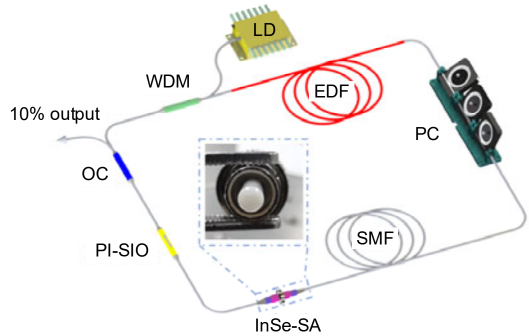

Fig. 4 Schematic of fiber laser setup

LD: laser diode; WDM: wavelength division multiplexer; EDF: erbium-doped fiber; PC: polarization controller; SMF: single-mode fiber; SA: saturable absorber; PI-ISO: polarization-independent isolator; OC: optical coupler

4 Experimental results and discussion

First, we insert the PVA film without InSe nanosheets between the fiber ferrules, and a continuous wave (CW) is observed. However, no mode-locked or Q-switched operations are observed by adjusting the pump power and the state of the PC.

Then, we insert the film of InSe-SA into the cavity. The CW operation is generated from the proposed EDF laser at a pump power of 5 mW. However, no pulsed operation is achieved by adjusting the state of the PC. Then, we gradually increase the pump power, and at the pump power of 35.8 mW the stable self-started mode-locked laser pulse train appears. As predicted by the pump hysteresis phenomenon, the single pulse mode-locked operation is also achieved by decreasing the pump power to 19 mW. Furthermore, by continuously increasing the pump power, stable mode-locked operation can be recorded with the pump power from 19 to 413 mW. The mode-locked operation is destroyed with a pump power larger than 413 mW. Fig. 5 provides the pulse characteristics of the passively mode-locked operation. Fig. 5a depicts an optical spectrum of the pulse. The central wavelength and 3-dB bandwidth are 1568.73 nm and 1.56 nm, respectively. Kelly sidebands at both sides of the spectrum, a typical feature of the soliton fiber lasers with negative dispersion, indicate that the pulses generated in the laser cavity are TS, which confirms that the laser works at the TS mode-locked operation. Fig. 5b provides the pulse train within 5 μs. The pulse interval of 577.7 ns between adjacent pulses corresponds to a 118.7 m long ring cavity, which further confirms that the laser works at the mode-locked operation. Fig. 5c shows the autocorrelation trace of a single pulse. The trace is well-fitted using a sech^2 profile. The full width at half maximum (FWHM) of the sech^2 profile is 3.18 ps, and thus the pulse duration is 3.18 ps×0.648=2.06 ps. The time-bandwidth product (TBP) is 0.401, which is larger than the standard value of 0.315, indicating that the pulse is slightly chirped. The RF spectrum measurement is conducted, and the fundamental frequency is 1.731 MHz with a signal-to-noise ratio (SNR) up to 53 dB, which is consistent with the pulse interval of 577.7 ns.

To further confirm the stability of the passive TS mode-locked operation, more measurements are executed. Fig. 6a provides a pulse train within 20 μs. No obvious intensity modulation is observed over such a long span. The optical spectra evolution within 1 h is shown in Fig. 6b. It shows that the spectrum is consistent over a long time. This shows that the fiber laser works in a highly stable TS mode-locked operation. Fig. 7 depicts the evolution of the average output

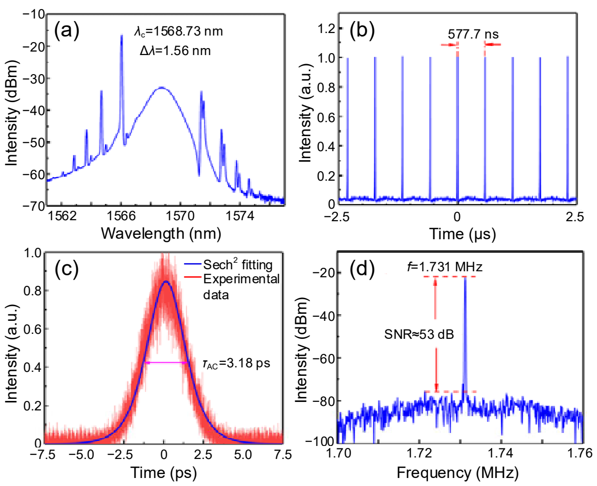

Fig. 5 Characteristics of mode-locked operation: (a) the spectrum with 3-dB bandwidth of 1.56 nm centered at 1568.73 nm; (b) the pulse interval of 577.7 ns between adjacent pulses; (c) autocorrelation trace for an output pulse with sech^2 fit and the FWHM being 3.18 ps; (d) the RF spectrum with a fundamental repetition rate of 1.731 MHz and the SNR greater than 53 dB

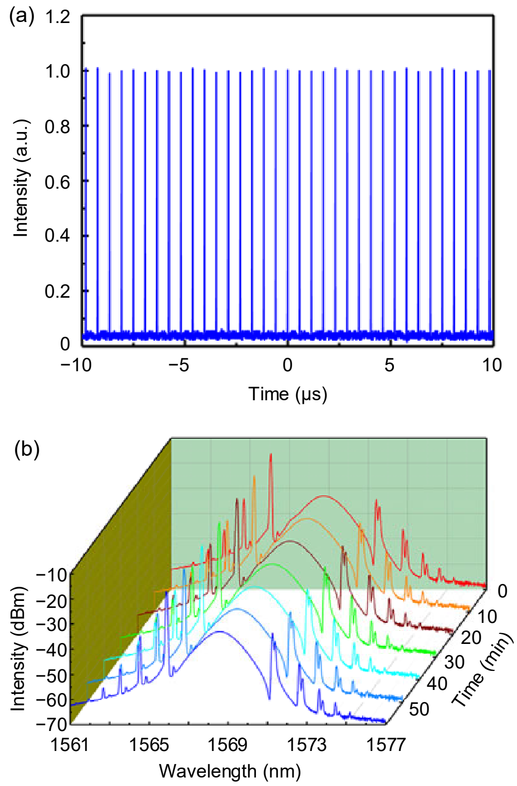

Fig. 6 Stability characteristics of the TS mode-locked operation: (a) the pulse train in a range of 20 μs; (b) optical spectra evolution within 60 min

power with an increase in the pump power. The average output power increases with the increase of the pump power under the TS mode-locked operation. The increasing trend is well fitted by a linear line, which indicates that the average output power linearly increases. The maximum average output power is 16.4 mW at a pump power of 413 mW. To verify the effect of the InSe-SA, we remove the SA from the laser cavity. Only the CW laser can be obtained, no matter how the pump power is adjusted and regardless of the state of PC. This proves that the mode-locked operation of the fiber laser is attributed to InSe-SA.

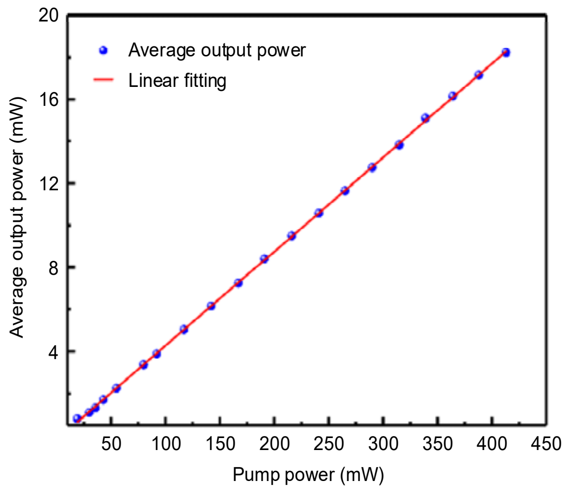

Fig. 7 The evolution of the average output power with the increase of the pump power

Table 1 systematically summarizes the performance of the fiber lasers based on In_2Se_3 or InSe as SA. Overall, In_2Se_3 and InSe are demonstrated for passively mode-locked and Q-switched operations at 1, 1.5, and 2 μm. The In_2Se_3-SA-based fiber lasers have picosecond level (Zhang WF et al., 2020) and even femtosecond level (Xu NN et al, 2020) TS pulses. However, the pulse durations of the reported InSe-SA-based fiber lasers are at the nanosecond level (Mudd et al., 2013; Quereda et al., 2016). The proposed fiber laser can generate a TS pulse with a pulse duration of 2.06 ps. This is beneficial for improving the peak intensity of the ultrashort pulse.

5 Conclusions

In summary, favorable performance in the generation of TS lasers employing InSe as SA has been experimentally demonstrated. InSe-PVA film has been prepared by InSe nanosheets solution and PVA solution. The nonlinear absorption properties of the InSe-SA have been investigated, showing a typical saturable absorption property. The nonsaturable absorption, modulation depth, and saturation intensity are 37.5%, 9.55%, and 1.68 MW/cm^2, respectively. The EDF laser has been designed and constructed by employing InSe-PVA film as SA. TS pulses centered at 1568.73 nm with a pulse duration of 2.06 ps have been obtained. The average output power increases

Table 1 Comparison of different In_2Se_3 or InSe based SA fiber lasers

Material	Material fabrication	SA fabrication	Modulation depth (%)	Operation	Central wavelength (nm)	Pulse duration	Reference
In_2Se_3	Mechanical exfoliation	Sandwiched	14.6	Mode-locked	1503.8	5.79 ps	Ahmad et al. (2018a)
In_2Se_3	Mechanical exfoliation	Sandwiched	22.48	Q-switched	Tunable	Tunable	Ahmad et al. (2018b)
In_2Se_3	Magnetron-sputtering deposition	Microfiber	4.5 6.9	TS TS	1565 1932	276 fs 1.02 ps	Yan et al. (2018)
In_2Se_3	LPE	Sandwiched	14	TS	Switchable	1.88/1.76 ps	Wang GM et al. (2019)
InSe	LPE	Microfiber	3.4	Q-switched	Tunable	Tunable	Xu NN et al. (2018)
InSe	LPE	Sandwiched	4.2	Mode-locked	1068.36	1.37 ns	Xu NN et al. (2018)
InSe	LPE	Sandwiched	16.5	Mode-locked	–	389.2 ns	Fu et al. (2019)
InSe	LPE	Sandwiched	9.55	TS	1568.73	2.06 ps	This work

SA: saturable absorber; LPE: liquid phase exfoliation; TS: traditional soliton linearly with the increase of the pump power. The study further shows that InSe is a promising material for developing ultrafast optoelectronics devices.

Contributors

Wenfei ZHANG designed the research. Xiaojuan LIU and Guomei WANG processed the data. Mingxiao ZHU drafted the manuscript. Kezhen HAN and Huanian ZHANG helped organize the manuscript. Wenfei ZHANG and Huanian ZHANG revised and finalized the paper.

Compliance with ethics guidelines

Xiaojuan LIU, Guomei WANG, Mingxiao ZHU, Kezhen HAN, Wenfei ZHANG, and Huanian ZHANG declare that they have no conflict of interest.

References

Ahmad H, Reduan SA, Ooi SI, et al., 2018a. Mechanically exfoliated In_2Se_3 as a saturable absorber for mode-locking a thulium-doped fluoride fiber laser operating in S-band. *Appl Opt*, 57(24):6937-6942. https://doi.org/10.1364/AO.57.006937

Ahmad H, Zulkifli AZ, Yasin M, et al., 2018b. In_2Se_3 saturable absorber for generating tunable Q-switched outputs from a bismuth-erbium doped fiber laser. *Laser Phys Lett*, 15(11):115105. https://doi.org/10.1088/1612-202x/aae13b

Bao QL, Zhang H, Wang Y, et al., 2009. Atomic-layer graphene as a saturable absorber for ultrafast pulsed lasers. *Adv Funct Mater*, 19(19):3077-3083. https://doi.org/10.1002/adfm.200901007

Chen JM, Fan TJ, Xie ZJ, et al., 2020. Advances in nanomaterials for photodynamic therapy applications: status and challenges. *Biomaterials*, 237:119827. https://doi.org/10.1016/j.biomaterials.2020.119827

Chen Y, Jiang GB, Chen SQ, et al., 2015. Mechanically exfoliated black phosphorus as a new saturable absorber for both Q-switching and mode-locking laser operation. *Opt Expr*, 23(10):12823-12833. https://doi.org/10.1364/OE.23.012823

Feng W, Zheng W, Gao F, et al., 2016. Sensitive electronic-skin strain sensor array based on the patterned two-dimensional α-In_2Se_3. *Chem Mater*, 28(12):4278-4283. https://doi.org/10.1021/acs.chemmater.6b01073

Fu SS, Li JJ, Zhang SS, et al., 2019. Large-energy mode-locked Er-doped fiber laser based on indium selenide as a modulator. *Opt Mater Expr*, 9(6):2662-2671. https://doi.org/10.1364/OME.9.002662

Ge YQ, Huang WC, Yang FM, et al., 2019. Beta-lead oxide quantum dot (β-PbO QD)/polystyrene (PS) composite films and their applications in ultrafast photonics. *Nanoscale*, 11(14):6828-6837. https://doi.org/10.1039/c9nr01112a

Goda K, Jalali B, 2013. Dispersive Fourier transformation for fast continuous single-shot measurements. *Nat Photon*, 7(2):102-112. https://doi.org/10.1038/nphoton.2012.359

Guo B, Wang SH, Wu ZX, et al., 2018. Sub-200 fs soliton mode-locked fiber laser based on bismuthene saturable absorber. *Opt Expr*, 26(18):22750-22760. https://doi.org/10.1364/OE.26.022750

Guo B, Xiao QL, Wang SH, et al., 2019. 2D layered materials: synthesis, nonlinear optical properties, and device applications. *Laser Photon Rev*, 13(12):1800327. https://doi.org/10.1002/lpor.201800327

Guo J, Zhao JL, Huang DZ, et al., 2019. Two-dimensional tellurium-polymer membrane for ultrafast photonics. *Nanoscale*, 11(13):6235-6242. https://doi.org/10.1039/C9NR00736A

Guo QX, Pan J, Liu YJ, et al., 2019. Output energy enhancement in a mode-locked Er-doped fiber laser using CVD-Bi_2Se_3 as a saturable absorber. *Opt Expr*, 27(17): 24670-24681. https://doi.org/10.1364/OE.27.024670

Guo SY, Zhang YP, Ge YQ, et al., 2019. 2D V-V binary materials: status and challenges. *Adv Mater*, 31(39): 1902352. https://doi.org/10.1002/adma.201902352

Hu QY, Zhang XY, Li ZJ, et al., 2019. High-order harmonic mode-locked Yb-doped fiber laser based on a $SnSe_2$ saturable absorber. *Opt Laser Technol*, 119:105639. https://doi.org/10.1016/j.optlastec.2019.105639

Huang D, Swanson EA, Lin CP, et al., 1991. Optical coherence tomography. *Science*, 254(5035):1178-1181. https://doi.org/10.1126/science.1957169

Huang WC, Jiang XT, Wang YZ, et al., 2018. Two-dimensional beta-lead oxide quantum dots. *Nanoscale*, 10(44):20540-20547. https://doi.org/10.1039/C8NR07788F

Huang WC, Zhang Y, You Q, et al., 2019. Enhanced photodetection properties of tellurium@selenium roll-to-roll nanotube heterojunctions. *Small*, 15(23):1900902. https://doi.org/10.1002/smll.201900902

Jhon YI, Koo J, Anasori B, et al., 2017. Metallic MXene saturable absorber for femtosecond mode-locked lasers. *Adv Mater*, 29(40):1702496. https://doi.org/10.1002/adma.201702496

Jiang XT, Liu SX, Liang WY, et al., 2018. Broadband nonlinear photonics in few-layer MXene $Ti_3C_2T_x$ (T=F, O, or OH). *Laser Photon Rev*, 12(2):1700229. https://doi.org/10.1002/lpor.201700229

Lei SD, Ge LH, Najmaei S, et al., 2014. Evolution of the electronic band structure and efficient photo-detection in atomic layers of InSe. *ACS Nano*, 8(2):1263-1272. https://doi.org/10.1021/nn405036u

Li D, Jussila H, Karvonen L, et al., 2015. Polarization and thickness dependent absorption properties of black phosphorus: new saturable absorber for ultrafast pulse generation. *Sci Rep*, 5(1):15899. https://doi.org/10.1038/srep15899

Li L, Pang LH, Zhao QY, et al., 2020. Niobium disulfide as a new saturable absorber for an ultrafast fiber laser. *Nanoscale*, 12(7):4537-4543. https://doi.org/10.1039/C9NR10873D

Liu GW, Zhang F, Wu TG, et al., 2019. Single-and dual-wavelength passively mode-locked erbium-doped fiber laser based on antimonene saturable absorber. *IEEE Photon J*, 11(3):1503011. https://doi.org/10.1109/JPHOT.2019.2917941

Liu GW, Lyu Y, Li ZW, et al., 2020. Q-switched erbium-doped fiber laser based on silicon nanosheets as saturable absorber. *Optik*, 202:163692. https://doi.org/10.1016/j.ijleo.2019.163692

Liu H, Zheng XW, Liu M, et al., 2014. Femtosecond pulse generation from a topological insulator mode-locked fiber laser. *Opt Expr*, 22(6):6868-6873. https://doi.org/10.1364/OE.22.006868

Liu JS, Li XH, Guo YX, et al., 2019. Harmonic mode-locking: $SnSe_2$ nanosheets for subpicosecond harmonic mode-locked pulse generation. *Small*, 15(38):1970206. https://doi.org/10.1002/smll.201970206

Liu WJ, Pang LH, Han HN, et al., 2017. Tungsten disulphide for ultrashort pulse generation in all-fiber lasers. *Nanoscale*, 9(18):5806-5811. https://doi.org/10.1039/c7nr00971b

Lu L, Liang ZM, Wu LM, et al., 2018. Few-layer bismuthene: sonochemical exfoliation, nonlinear optics and applications for ultrafast photonics with enhanced stability. *Laser Photon Rev*, 12(1):1700221. https://doi.org/10.1002/lpor.201700221

Luo ZC, Liu M, Guo ZN, et al., 2015. Microfiber-based few-layer black phosphorus saturable absorber for ultrafast fiber laser. *Opt Expr*, 23(15):20030-20039. https://doi.org/10.1364/OE.23.020030

Ma PF, Li JS, Zhang HN, et al., 2020. Preparation of high-damage threshold WS_2 modulator and its application for generating high-power large-energy bright-dark solitons. *Infrar Phys Technol*, 105:103257. https://doi.org/10.1016/j.infrared.2020.103257

Mao D, Li MK, Cui XQ, et al., 2018. Stable high-power saturable absorber based on polymer-black-phosphorus films. *Opt Commun*, 406:254-259. https://doi.org/10.1016/j.optcom.2016.11.027

Mudd GW, Svatek SA, Ren TH, et al., 2013. Tuning the bandgap of exfoliated InSe nanosheets by quantum confinement. *Adv Mater*, 25(40):5714-5718. https://doi.org/10.1002/adma.201302616

Niu KD, Chen QY, Sun RY, et al., 2017. Passively Q-switched erbium-doped fiber laser based on SnS_2 saturable absorber. *Opt Mater Expr*, 7(11):3934-3943. https://doi.org/10.1364/OME.7.003934

Niu KD, Sun RY, Chen QY, et al., 2018. Passively mode-locked Er-doped fiber laser based on SnS_2 nanosheets as a saturable absorber. *Photon Res*, 6(2):72-76. https://doi.org/10.1364/PRJ.6.000072

Quereda J, Biele R, Rubio-Bollinger G, et al., 2016. Strong quantum confinement effect in the optical properties of ultrathin α-In_2Se_3. *Adv Opt Mater*, 4(12):1939-1943. https://doi.org/10.1002/adom.201600365

Song YF, Chen S, Zhang Q, et al., 2016. Vector soliton fiber laser passively mode locked by few layer black phosphorus-based optical saturable absorber. *Opt Expr*, 24(23):25933-25942. https://doi.org/10.1364/oe.24.025933

Song YF, Liang ZM, Jiang XT, et al., 2017. Few-layer antimonene decorated microfiber: ultra-short pulse generation and all-optical thresholding with enhanced long term stability. *2D Mater*, 4(4):045010. https://doi.org/10.1088/2053-1583/aa87c1

Sotor J, Sobon G, Abramski KM, 2014a. Sub-130 fs mode-locked Er-doped fiber laser based on topological insulator. *Opt Expr*, 22(11):13244-13249. https://doi.org/10.1364/OE.22.013244

Sotor J, Sobon G, Macherzynski W, et al., 2014b. Black phosphorus saturable absorber for ultrashort pulse generation. *Appl Phys Lett*, 107(5):051108. https://doi.org/10.1063/1.4927673

Sun XL, Zhang BT, Yan BZ, et al., 2018. Few-layer $Ti_3C_2T_x$ (T=O, OH, or F) saturable absorber for a femtosecond bulk laser. *Opt Lett*, 43(16):3862-3865. https://doi.org/10.1364/OL.43.003862

Wang C, Wang L, Li XH, et al., 2019. Few-layer bismuthene for femtosecond soliton molecules generation in Er-doped fiber laser. *Nanotechnology*, 30(2):025204. https://doi.org/10.1088/1361-6528/aae8c1

Wang C, Xu JW, Wang YZ, et al., 2020. MXene (Ti_2NT_x): synthesis, characteristics and application as a thermo-optical switcher for all-optical wavelength tuning laser. *Sci China Mater*, in press. https://doi.org/10.1007/s40843-020-1409-7

Wang GM, Chen GW, Li WL, et al., 2019. Indium selenide as a saturable absorber for a wavelength-switchable vector-soliton fiber laser. *Opt Mater Expr*, 9(2):449-456. https://doi.org/10.1364/OME.9.000449

Wang GM, Zhang WF, Xing F, et al., 2020. Tin monoselenide based saturable absorbers for the generation of ultrashort pulses. *Infrar Phys Technol*, 108:103349. https://doi.org/10.1016/j.infrared.2020.103349

Wang MX, Zhang F, Wang ZP, et al., 2019. Liquid-phase exfoliated silicon nanosheets: saturable absorber for solid-state lasers. *Materials*, 12(2):201. https://doi.org/10.3390/ma12020201

Wu LM, Xie ZJ, Lu L, et al., 2018. Few-layer tin sulfide: a promising black-phosphorus-analogue 2D material with exceptionally large nonlinear optical response, high stability, and applications in all-optical switching and wavelength conversion. *Adv Opt Mater*, 6(2):1700985. https://doi.org/10.1002/adom.201700985

Wu Q, Jin X, Chen S, et al., 2019. MXene-based saturable absorber for femtosecond mode-locked fiber lasers. *Opt Expr*, 27(7):10159-10170. https://doi.org/10.1364/OE.27.010159

Xie ZJ, Zhang F, Liang ZM, et al., 2019. Revealing of the ultrafast third-order nonlinear optical response and enabled photonic application in two-dimensional tin sulfide. *Photon Res*, 7(5):494-502.

https://doi.org/10.1364/PRJ.7.000494

Xie ZJ, Fan TJ, An JS, et al., 2020. Emerging combination strategies with phototherapy in cancer nanomedicine. *Chem Soc Rev*, in press. https://doi.org/10.1039/D0CS00215A

Xing CY, Xie ZJ, Liang ZM, et al., 2017. 2D nonlayered selenium nanosheets: facile synthesis, photoluminescence, and ultrafast photonics. *Adv Opt Mater*, 5(24):1700884. https://doi.org/10.1002/adom.201700884

Xu NN, Yang WQ, Zhang HN, 2018. Nonlinear saturable absorption properties of indium selenide and its application for demonstrating a Yb-doped mode-locked fiber laser. *Opt Mater Expr*, 8(10):3092-3103. https://doi.org/10.1364/OME.8.003092

Xu NN, Ming N, Han XL, et al., 2019. Large-energy passively Q-switched Er-doped fiber laser based on CVD-Bi_2Se_3 as saturable absorber. *Opt Mater Expr*, 9(2):373-383. https://doi.org/10.1364/OME.9.000373

Xu NN, Ma PF, Fu SS, et al., 2020. Tellurene-based saturable absorber to demonstrate large-energy dissipative soliton and noise-like pulse generations. *Nanophotonics*, 9(9): 2783-2795. https://doi.org/10.1515/nanoph-2019-0545

Xu YH, Jiang XF, Ge YQ, et al., 2017. Size-dependent nonlinear optical properties of black phosphorus nanosheets and their applications in ultrafast photonics. *J Mater Chem C*, 5(12):3007-3013. https://doi.org/10.1039/C7TC00071E

Yan PG, Jiang ZK, Chen H, et al., 2018. α-In_2Se_3 wideband optical modulator for pulsed fiber lasers. *Opt Lett*, 43(18): 4417-4420. https://doi.org/10.1364/OL.43.004417

Yang WQ, Xu NN, Zhang HN, 2018. Nonlinear absorption properties of indium selenide and its application for demonstrating pulsed Er-doped fiber laser. *Laser Phys Lett*, 15(10):105101. https://doi.org/10.1088/1612-202X/aad896

Zhang H, Bao QL, Tang DY, et al., 2009. Large energy soliton erbium-doped fiber laser with a graphene-polymer composite mode locker. *Appl Phys Lett*, 95(14):141103. https://doi.org/10.1063/1.3244206

Zhang HN, Ma PF, Zhu MX, et al., 2020. Palladium selenide as a broadband saturable absorber for ultra-fast photonics. *Nanophotonics*, 9(8):2557-2567. https://doi.org/10.1515/nanoph-2020-0116

Zhang WF, Wang GM, Xing F, et al., 2020. Passively Q-switched and mode-locked erbium-doped fiber lasers based on tellurene nanosheets as saturable absorber. *Opt Expr*, 28(10):14729-14739. https://doi.org/10.1364/OE.392944

Zhao Y, Guo PL, Li XH, et al., 2019. Ultrafast photonics application of graphdiyne in the optical communication region. *Carbon*, 149:336-341. https://doi.org/10.1016/j.carbon.2019.04.075